Preprints, 4th IFAC Conference on
Advances in Proportional-Integral-Derivative Control
Almería, Spain | June 12-14, 2024

Improving the relay feedback identification by using a gain-changing non-linearity ⋆

Julio-Ariel Romero-Pérez * **Oscar Miguel-Escrig** *
José Sánchez-Moreno ** **Sebastián Dormido-Bencomo** **

* *Departamento de Ingeniería de Sistemas Industriales y Diseño, UJI, Castelló, Spain (romeroj@uji.es)*
** *Departamento de Informática y Automática, UNED, Madrid, Spain*

Abstract: This paper proposes the use of the gain-changing non-linearity to improve the estimation of the ultimate point, which is used in many auto-tuning algorithm of PID controllers. The experiments for identification are similar to the relay feedback, therefore some well known advantages of this kind of experiments are maintained while the estimation error is significantly reduced. The identification method is evaluated with a batch of system dynamics, providing suitable results in all cases, which proves the validity of the approach.

Keywords: Identification for control, relay feedback experiment, auto-tune, PID

1. INTRODUCTION

PID controllers are used in most of the industrial control applications due to its simplicity and robustness. One of the main features that boosts the application of PID in industry is the availability of auto-tuning algorithms which facilitate the use of the control devices by automatically calculating the controller parameters after a simple experiment on the control loop.

Many tuning and auto-tuning methods use the ultimate gain and frequency to obtain the controller parameters. The ultimate gain is the value of gain for which a closed-loop system start to oscillate with constant amplitude, and the frequency of these oscillations is the ultimate frequency. This information can be easily obtained through a feedback relay experiment, where an oscillatory response is induced in the loop when substituting the PID by a relay. The amplitude of the oscillations can be controlled by the relay configuration parameters (amplitude and hysteresis), which is the main advantage of this approach respect to the original method proposed by Ziegler and Nichols, consisting on replacing the controller by a gain and increase it until the oscillatory behavior is obtained, Ziegler and Nichols (1942).

Since the relay feedback experiment was proposed in Åström and Hägglund (1984), a lot of work have been carried out to obtain more accurate results from it. In this sense, it is worth noting that the equation to calculate the ultimate gain is obtained by applying the describing function (DF) technique to the control loop with relay feedback. It is well known, that the DF methodology assumes the non-linearity input to be a pure sinusoidal signal, neglecting the effect of the higher order harmonics in the oscillatory response of the system due to the limit cycle induced by the relay feedback. This assumption is valid if the process to identify is filtering enough, but fails if this condition is not fulfilled.

The existence of higher-order harmonics in the input to the non-linearity significantly impacts the accuracy of estimations based on the DF (Describing Function) approach. Therefore, the estimation error could be reduced by considering the effect of these harmonics in the calculations, as proposed in Miguel-Escrig and Romero-Pérez (2022). Alternatively, the effect of higher order harmonics in the system response can be reduced in order to decrease the estimation error when applying the DF technique. This is the rationale behind the use of the gain-changing non-linearity for identification proposed in this paper.

The use of the gain-changing non-linearity is inspired by the results presented in Tan et al. (2006) and Yu (2006), where the preload-relay and the saturation-relay are proved to improve the ultimate gain and frequency identification respect to the relay feedback experiments. These methods attempt to reduce the effect of neglecting the higher order harmonics by introducing slight modifications to the original relay test and calculations. The preload-relay consists of a relay in parallel with a gain, and the saturation-relay input/output characteristic corresponds to the saturation non-linearity. These two relay configurations are particular cases of the gain-changing non-linearity. Here we prove that intermediate configurations, defined by the slopes of the lines conforming the non-linearity, can significantly reduce the identification error.

The rest of the paper is organized as follows. The next section describes the gain-changing non-linearity and introduces the parameters that define its input/output characteristic. Section 3 analyzes the effect of introducing this non-linearity in a control loop, concretely, the generation of higher order harmonic is studied, since these harmonics

⋆ This work was supported by the research project UJI-B2021-45/21I596 from Universitat Jaume I, Spain, and by the State Research Agency under projects PID2020-112658RBI00 and PID2022-1398187OB-I00.

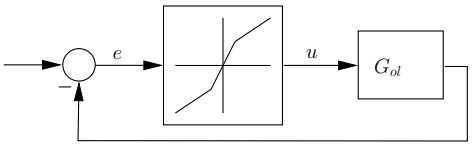

Fig. 1. Closed loop system with gain-changing non-linearity.

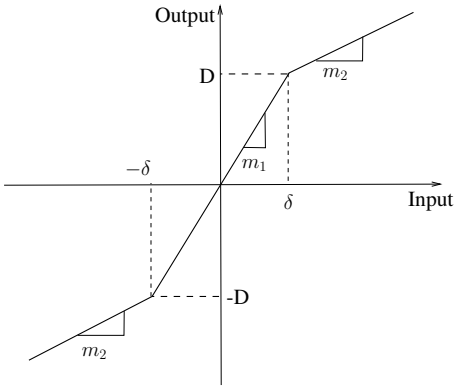

Fig. 2. Intput-output characteristic of the gain-changing non-linearity.

strongly affect the accuracy of ultimate gain and frequency estimation. The identification procedure is proposed in Section 4, after which, some clarifying simulation examples are introduced in Section 5. Finally, Section 6 summarizes the conclusions of the paper.

2. GAIN-CHANGING NON-LINEARITY

The closed loop systems including a gain-changing non-linearity is depicted in Figure 1. Figure 2 shows the input-output characteristic of the gain-changing non-linearity, which is fully defined by the slopes m_1 and m_2 and the points $(-\delta, -D)$ and (δ, D). A wide range of non-linearities can be obtained by varying m_1 and m_2, for instance, a relay is obtained for $m_1 = \infty$ and $m_2 = 0$, a saturation relay results from $0 < m_1 < \infty$ and $m_2 = 0$, and a preload-relay is shaped with $m_1 = \infty$ and $0 < m_2 < \infty$.

The classical method of relay feedback identification relies on the DF technique. The oscillation induced by the relay is predicted to take place in the intersection point between the open loop transfer function ($G_{ol}(j\omega)$) and the negative inverse of the relay's describing function, given by the equation $-1/N(A) = \frac{\pi A}{4D}$, where $N(A)$ is the describing function and A and D are the amplitudes of oscillation and relay, respectively. In the intersection point, the following equation is fulfilled, $|G_{ol}(j\omega_o)| = \frac{\pi A_o}{4D}$. Using this equation, $|G_{ol}(j\omega_o)|$ can be estimated by measuring the amplitude A_o of the oscillation, whose frequency corresponds to ω_o.

The DF of the gain-changing non-linearity is given by equation (1), Gelb and VanderVelde (1968). In the real-imaginary plane, the negative inverse of $N(A)$ corresponds to a line segment over the real axis between the values $-1/m_2$ and $-1/m_1$. This is an important difference respect to the relay DF, whose negative inverse extends over the negative part of the real axis, which is a particular case of the gain-changing non-linearity when $m_1 = \infty \Rightarrow -1/m_1 = 0$ and $m_2 = 0 \Rightarrow -1/m_2 = \infty$.

$$N(A) = \frac{2(m_1 - m_2)}{\pi}\left[\text{asin}\left(\frac{\delta}{A}\right) + \frac{\delta}{A}\sqrt{1 - \left(\frac{\delta}{A}\right)^2}\right] + m_2 \tag{1}$$

Depending on the relation between m_1 and m_2, two situations are possible which are shown in Figure 3. The arrows over the $-1/N(A)$ locus indicate the direction of increasing A. If $m_1 > m_2$, the increment of A moves the system to a stable configuration (region to the left of G_{ol}) in which the amplitude decays to its original value A_o; whereas the decrement of A moves the system to an unstable configuration (region encircled by G_{ol}) where the amplitude grows to its original value A_o. Therefore, the limit cycle obtained when $m_1 > m_2$ is stable. Following a similar analysis, it can be settled that the limit cycle induced by the gain-changing non-linearity when $m_1 < m_2$ is unstable since variations on the oscillation amplitude are not canceled, but amplified by the system response.

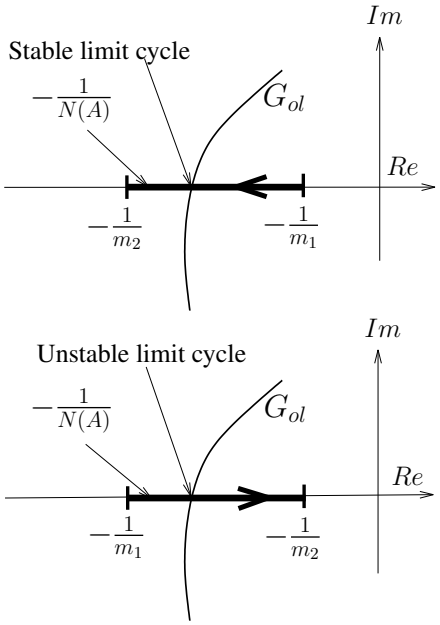

Fig. 3. Stable and unstable limit cycles induced by the gain-changing non-linearity.

From the previous discussion, it is clear that for identification of the ultimate gain and frequency, the gains of the non-linearity must fulfill the condition $m_1 > m_2$, in order to obtain an oscillatory behavior. The question that rises immediately is what values of m_1 and m_2 are the best choice to reduce the estimation error as much as possible? In the next section the answer to this question is addressed.

3. HARMONICS GENERATION

One of the main source of error when estimating the ultimate gain and frequency using the classical relay feedback method is the presence of higher order harmonics in the oscillatory response of the actual system, which are neglected in the DF approach. Therefore, the estimation error can be reduced by decreasing the amplitude of these harmonics respect to the fundamental one. In cases when the plant to identify does not fulfill the filtering condition

that allows to oversight the higher harmonics, the proper design of the non-linearity, instead of using a single relay, might contribute to this end.

For the gain-changing non-linearity, the ratio between the amplitude of harmonics with order $k = 3, 5, 7, \cdots$ and the fundamental harmonic in the output, when considering a sinusoidal input $A\sin(\omega t)$, is given by equation (2), where $\beta = m_2/m_1$. The even harmonics cancel in the Fourier series representation of a signal processed through the gain-changing due to the symmetric nature of this non-linearity.

$$\frac{A_k}{A_1} = \frac{4(1-\beta)}{k(1-k^2)} \times \frac{\left(\frac{\delta}{A}\cos\left(k\sin^{-1}\left(\frac{\delta}{A}\right)\right) - k\sin\left(k\sin^{-1}\left(\frac{\delta}{A}\right)\right)\sqrt{1-\frac{\delta^2}{A^2}}\right)}{\left((1-\beta)\left(2\frac{\delta}{A}\sqrt{1-\frac{\delta^2}{A^2}} + 2\sin^{-1}\left(\frac{\delta}{A}\right)\right) + \pi\beta\right)} \tag{2}$$

Using the previous equation, the total effect of the higher order harmonics respect to the fundamental one, expressed in percentage, can be calculated by equation (3). It should be noted that values of A_T near to zero indicate the prevalence of the main harmonic over the higher order components, and consequently, a better estimation of the critical point based on the DF approach.

$$A_T = \frac{\sum_{k=3,5,\ldots}^{\infty} |A_k|}{|A_1|} \times 100 = \sum_{k=3,5,\ldots}^{\infty} \left|\frac{A_k}{A_1}\right| \times 100 \tag{3}$$

The surface defined by equation (3) is shown in Figure 4, furthermore the contour lines of this surface are depicted in Figure 5. It can be seen that A_T is strongly affected by both β and δ/A. It is worth noting that, despite the value of δ/A, A_T decreases rapidly as β increases. The highest value of A_T correspond to $\beta = m_2/m_1 = 0$, that is, for non-linearity configurations with $m_2 = 0$, which include the cases of classical and saturation relay. On the other hand, for $\beta = 1$ the amplitudes of higher order harmonics are zero. This result is coherent with the fact that for $\beta = 1$ the non-linearity is transformed into a single gain of value m_1, and consequently, the output to a sinusoidal input has only a first order harmonic corresponding to the input amplification: $m_1 A\sin(\omega t)$.

Remark 1. A very important feature shown in Figure 5 is that for $\beta > 0.6$ the values of A_T are lower than 10%, disregarding the value of δ_A. Based on this fact, it is reasonable to consider that non-linearity configurations with $\beta > 0.6$ are more suitable for identification through the DF approach than those with smaller values of β, since the former reduce the impact of the superior harmonics in the output. This property of the gain-changing non-linearity will be used in the identification procedure proposed in the next section.

4. IDENTIFICATION PROCEDURE

The goal of the identification procedure is to estimate the ultimate gain taking advantages of the gain-changing non-linearity properties commented in the previous sections. From Remark 1, the best configurations for identification

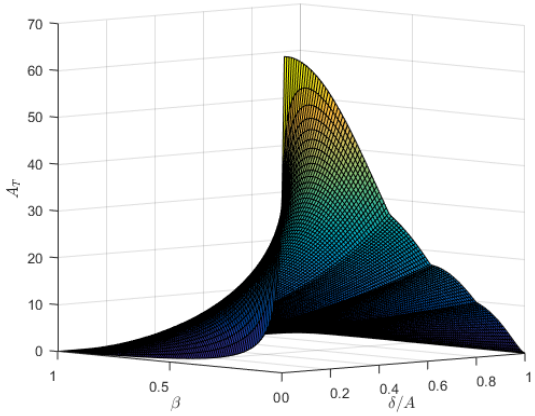

Fig. 4. Surface of A_T as a function of δ/A and $\beta = m_2/m_1$.

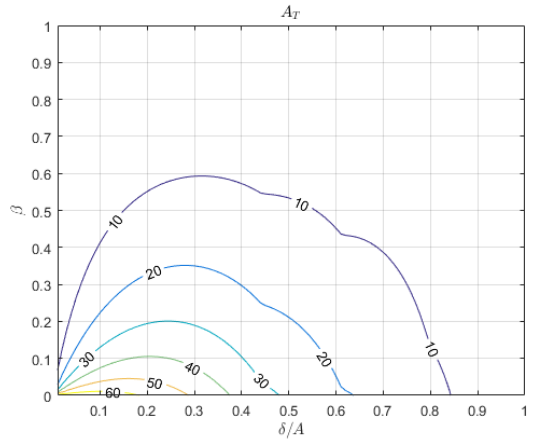

Fig. 5. Contours of A_T as a function of δ/A and $\beta = m_2/m_1$.

are those with $m_2/m_1 = \beta > 0.6$. However, according to Figure 3, the locus of $-1/N(a)$ over the real axis is completely defined by the two slopes, the locus being narrower as m_1 and m_2 are closer, that is, as β increase. These two facts lead the selection of m_1 and m_2 to reduce the effect of higher order harmonics, and at the same time, guarantee a wide enough locus of $-1/N(a)$ to assure its intersection with $G_{ol}(j\omega)$, in order to obtain limit cycle oscillations.

Because the plant model is unknown a priori, not information is available about the intersection point of $G_{ol}(j\omega)$ with the real axis, and consequently, proper values of m_1 and m_2 which guarantee both $\beta > 0.6$ and the intersection between $G_{ol}(j\omega)$ and $1/N(A)$ can not be assigned at the beginning of the experiment. To overcome this issue, the values of m_1 and m_2 must be initially fixed to assure the intersection between G_{ol} and $-1/N(A)$, no matter where the intersection take place. To this end, the configuration of the non-linearity should approximate an ideal relay, whose negative inverse of the describing function extends over the negative part of the real axis. Therefore, an experiment with $m_1 = \infty$ and $m_2 = 0$ is carried on in the first stage of the identification procedure. Using the amplitude of the oscillation A_o, an initial estimation of $|G_{ol}(j\omega_o)|$ can be obtained by the equation:

$$|\hat{G}_{ol}(j\omega_o)| = \frac{\pi A_o}{4D}. \quad (4)$$

To improve the initial estimation of $|G_{ol}(j\omega_o)|$, the values of m_1 and m_2 need to be recalculated to develop a second experiment with a reduced impact of the higher order harmonics, that is, for $m_2/m_1 = \beta \geqslant 0.6$. Furthermore, its values must assure the intersection between G_{ol} and $-1/N(A)$ to guarantee stable limit cycle oscillations for the second phase of the identification. In this sense, assuming that the actual critical point is relatively close to $\hat{G}_{ol}(j\omega_o)$, it is feasible to obtain m_1 and m_2 through the following equations:

$$m_1 = \frac{k_1}{|\hat{G}_{ol}(j\omega_o)|},\ k_1 > 1 \quad (5)$$

$$m_2 = \frac{k_2}{|\hat{G}_{ol}(j\omega_o)|},\ k_2 < 1 \quad (6)$$

The parameters k_1 and k_2 define both the range of $-1/N(A)$ over the real axis and the value of β, therefore its choice is a trade-off between reducing the effect of high order harmonics and guarantee the existence of a limit cycle. Since the initial estimation of $|G_{ol}(j\omega_o)|$ is carried out from a relay experiment, a reasonable selection of k_1 and k_2 must take into account the estimation error introduced by this kind of experiment in order to assure the intersection between G_{ol} and $-1/N(A)$.

In order to get some information about the magnitude of the estimation error introduced by the relay feedback experiment, its value has been calculated for the batch of 134 models presented in the Appendix A. This test batch was firstly proposed in Åström and Hägglund (2006), and it includes models with multiple poles, complex and real poles, integrators, non-minimal phase and time delays.

The results are shown in Figure 6. As expected, the largest errors correspond to low filtering models, because of the discordance with the DF assumption about the effect of higher order harmonics. It should be noted that in the worst cases, the relative error is under 25%, so this value could be considered as a reasonable upper bound of the estimation error in the early stage of the identification procedure, and consequently, the actual critical point is expected to be in the range $[-1.25|\hat{G}_{ol}(j\omega_o)|, -0.75|\hat{G}_{ol}(j\omega_o)|]$. Therefore, taking into account that for the gain-changing non-linearity the locus of $-\frac{1}{N(A)}$ is limited to the interval $[-\frac{1}{m_2}, -\frac{1}{m_1}]$, the equations to calculate m_1 and m_2 are as follows:

$$m_1 = \frac{1}{0.75|\hat{G}_{ol}(j\omega_o)|} \quad (7)$$

$$m_2 = \frac{1}{1.25|\hat{G}_{ol}(j\omega_o)|} \quad (8)$$

From the previous expressions, the values of k_1 and k_2 of equations (5) and (6) are deduced to be $\frac{1}{0.75}$ and $\frac{1}{1.25}$, respectively.

Equations (7) and (8) lead to $\beta = m_2/m_1 = 0.75/1.25 = 0.6$. According to Figure 5, this value of β guarantees a relatively low influence of the higher order harmonics in the non-linearity output, concretely less than the 10% respect to the fundamental component. In the identification

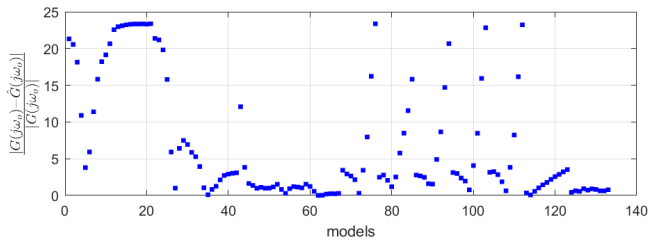

Fig. 6. Relative error of the estimated oscillation points with the conventional relay method applied to the batch of models in Appendix A.

procedure, the values of m_1 and m_2 can be calculated from the amplitude of the relay induced oscillations (A_o) using the following expressions, which are obtained by substituting equation (4) in (7) and (8).

$$m_1 = \frac{5.3D}{\pi A_o} \quad (9)$$

$$m_2 = \frac{3.2D}{\pi A_o} \quad (10)$$

Using these values of m_1 and m_2, a new experiment is developed at the end of which an improved estimation of $|G_{ol}(j\omega)|$ is calculated as follows:

$$|\hat{G}_{ol}(j\omega_o)| = \frac{1}{N(A_o)} \quad (11)$$

where $N(A_o)$ is given by equation (1), being A_o the amplitude of the oscillation induced by the gain-changing non-linearity. The rest of parameters in the equation (1), that is m_1, m_2 and δ, are set to the values used for this last experiment.

The identification procedure can be summarized in the following steps:

(1) Configure the gain-changing non-linearity as a relay, that is, set $m_1 = \infty$ and $m_2 = 0$. The relay amplitude D should assure a reasonable amplitude of the induced oscillation.
(2) Carry out the relay feedback experiment with the configuration of the non-linearity fixed in the step 1. Once the system presents a stable oscillation, measure its amplitude A_o.
(3) Calculate the value of m_1 and m_2 using equations (7) and (8), and reconfigure the gain-changing non-linearity with these values.
(4) Develop a second experiment with the new configuration of the non-linearity. Once the system presents a stable oscillation, measure its amplitude A_o.
(5) Calculate the value of $|G_{ol}(j\omega_o)|$ by equation (11).

Once finalized the experiment 2, its result can be used for tuning a PID or another kind of controller.

5. SIMULATION EXAMPLES

In this section several simulation examples are introduced to clarify the identification procedure and to verify its effectiveness on estimating the ultimate gain. It is worth noting that in all the examples the model of the plant is unknown from the identification algorithm point of view. In fact, the goal of the procedure is to estimate

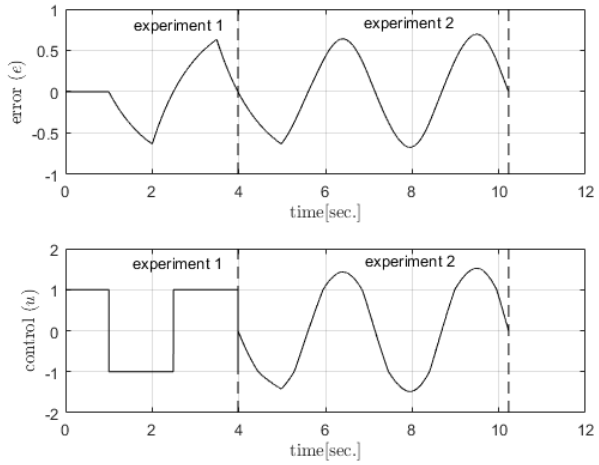

Fig. 7. Time response during the experiment with G_1.

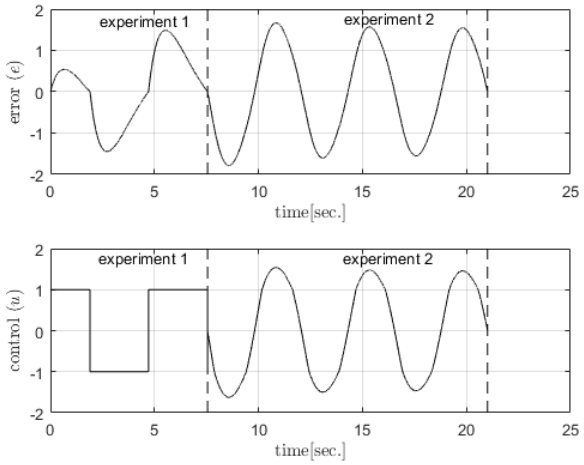

Fig. 8. Time response during the experiment with G_5.

the critical gain without previous information about the system dynamics.

Five systems with very different dynamic behavior are considered, whose models are given by equations (12) to (16). Concretely, low and high order systems, with and without time delay, as well as non-minimum phase dynamic are studied when applied the proposed procedure. In all cases the relay amplitude D is assumed to be 1.

$$G_1(s) = \frac{e^{-1s}}{1s+1} \tag{12}$$

$$G_2(s) = \frac{e^{-1s}}{(1s+1)^2} \tag{13}$$

$$G_3(s) = \frac{1}{(1s+1)^5} \tag{14}$$

$$G_4(s) = \frac{1}{(s+1)(0.5s+1)(0.25s+1)(0.125s+1)} \tag{15}$$

$$G_5(s) = \frac{-2(s-0.5)}{(s+1)^2} \tag{16}$$

Figures 7 and 8 show the time response of error (e) and control (u) signals during the identification for systems G_1 and G_5, which have been selected to illustrate the performance of the procedure. In both figures the vertical dashed lines indicate the final of each experiment. As can be seen from the plot of u, experiment 1 corresponds to a relay feedback test, which is attained by setting $m_1 = \infty$ and $m_2 = 0$ in the non-linearity. At the end of experiment 1, the non-linearity is reconfigured by recalculating the slopes m_1 and m_2, then experiment 2 begins, which finishes with the calculation of $|G_{ol}(j\omega_o)|$.

It should be noted that, as a result of the non-linearity configuration with the suitable values of m_1 and m_2 proposed in the procedure, e and u are almost sinusoidal signals throughout the experiment 2. This fact reveals the reduced amplitude of the higher order harmonics, in contrast with experiment 1, where the signals are far from being sinusoidal.

The results of the identification for models G_1 and G_5 are depicted in Figures 9 and 10, where the polar plot of the open loop transfer functions ($G_1(j\omega)$ and $G_2(j\omega)$) as well

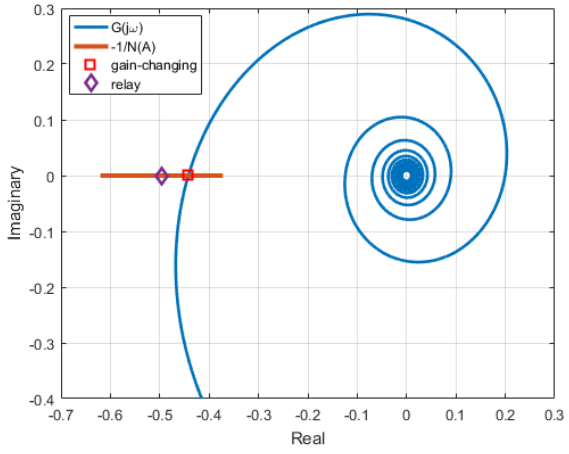

Fig. 9. Polar plot with the identification results for G_1.

as the frequency response points estimated using both a relay experiment and the proposed procedure are shown. As can be seen, in both cases the use of the gain-changing non-linearity allows improving the estimation significantly. The locus of $-1/N(A)$, also represented in the figures, are wide enough to guarantee the intersection with $G_{ol}(j\omega)$. It can be observed that the plots of $-1/N(A)$ are centered in the point obtained from the relay experiments, extending to left and right in a range of $\pm 25\%$, that according to Figure 6 can be considered the upper bound of the estimation error from relay feedback experiments. Therefore, the actual critical point is expected to be within this range, which can indeed be seen in the figures.

Models G_1 to G_5 have been used to compare the gain-changing non-linearity identification procedure presented in this paper with other methods previously proposed in the literature. Concretely we consider the classical relay feedback, as well as two improved versions of the relay type experiments: the preload-relay Tan et al. (2006) and saturation-relay Yu (2006). The relative error between the identification results obtained with each method and the actual critical point of these systems were calculated. The results are summarized in Table 5. As can be seen, the gain-changing method provides the lowest relative estima-

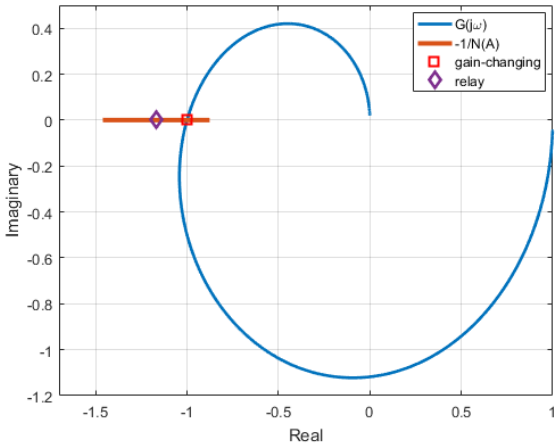

Fig. 10. Polar plot with the identification results for G_5.

tion error for all the systems. Furthermore, the improvement in the ultimate point identification is higher for low order systems. This fact is coherent with the significant presence of non-fundamental harmonics in these systems whose effect is minimized when introducing the gain-changing non-linearity with the proper values of slopes m_1 and m_2 obtained with the proposed algorithm.

Table 1. Relative error in the ultimate point estimation.

Method	G_1	G_2	G_3	G_4	G_5
Gain-changing	0.10	0.13	0.09	0.06	0.21
Simple relay	12.24	5.92	1.46	2.83	16.84
Preload relay	4.90	3.02	0.70	1.29	7.93
Saturation relay	1.38	0.70	0.42	0.69	0.79

6. CONCLUSIONS

This article presents a new method to estimate the ultimate gain and frequency for tuning PID controllers. The procedure includes a novel type of experiment based on the use of the gain-changing non-linearity, which allows the estimation error to be reduced. Several simulation examples show the advantages of the proposal over previous approaches. The procedure can be easily implemented as part of automatic PID tuning algorithms to improve their performance.

REFERENCES

Åström, K.J. and Hägglund, T. (1984). Automatic tuning of simple regulators with specifications on phase and amplitude margins. *Automatica*, 20(5), 645–651. doi: 10.1016/0005-1098(84)90014-1.

Åström, K. and Hägglund, T. (2006). *Advanced PID Control*. ISA-The Instrumentation, Systems, and Automation Society.

Gelb, A. and VanderVelde, W.E. (1968). *Multiple-Input Describing Functions and Nonlinear System Design*. New York, NY, USA: McGraw-Hill.

Miguel-Escrig, O. and Romero-Pérez, J.A. (2022). Improving the identification from relay feedback experiments. *Automatica*, 135, 109987. doi: https://doi.org/10.1016/j.automatica.2021.109987.

Tan, K., Lee, T., Huang, S., Chua, K., and Ferdous, R. (2006). Improved critical point estimation using a preload relay. *Journal of Process Control*, 16(5), 445–455. doi: https://doi.org/10.1016/j.jprocont.2005.09.004.

Yu, C.C. (2006). *Autotuning of PID Controllers. A Relay Feedback Approach*, chapter Improved Relay Feedback, 75–96. Springer, 2nd edition.

Ziegler, J.G. and Nichols, N.B. (1942). Optimum Settings for Automatic Controllers. *Trans. ASME.*, 64(8), 759–765.

Appendix A. BATCH OF MODELS

Models 1 to 21 in Figure 6:

$$G(s) = \frac{e^{-s}}{Ts+1}, \tag{A.1a}$$

$T = 0.02, 0.05, 0.1, 0.2, 0.3, 0.5, 0.7, 1,$
$1.3, 1.5, 2, 4, 6, 8, 10, 20, 50, 100, 200, 500, 1000$

Models 22 to 42 in Figure 6:

$$G(s) = \frac{e^{-s}}{(1+sT)^2}, \tag{A.1b}$$

$T = 0.01, 0.02, 0.05, 0.1, 0.2, 0.3, 0.5, 0.7, 1,$
$1.3, 1.5, 2, 4, 6, 8, 10, 20, 50, 100, 200, 500$

Models 43 to 52 in Figure 6:

$$G(s) = \frac{e^{-s}}{(s+1)(Ts+1)^2}, \tag{A.1c}$$

$T = 0.005, 0.01, 0.02, 0.05, 0.1, 0.2, 0.5, 2, 5, 10$

Models 53 to 58 in Figure 6:

$$G(s) = \frac{1}{(s+1)^n}, \tag{A.1d}$$

$n = 3, 4, 5, 6, 7, 8$

Models 59 to 67 in Figure 6:

$$G(s) = \frac{1}{(s+1)(\alpha s+1)(\alpha^2 s+1)(\alpha^3 s+1)}, \tag{A.1e}$$

$\alpha = 0.1, 0.2, 0.3, 0.4, 0.5, 0.6, 0.7, 0.8, 0.9$

Model 68 to 76 in Figure 6:

$$G(s) = \frac{1}{s(1+sT_1)}e^{-sL_1}, \quad T_1 + L_1 = 1, \tag{A.1f}$$

$L_1 = 0.01, 0.02, 0.05, 0.1, 0.3, 0.5, 0.7, 0.9, 1$

Model 77 to 113 in Figure 6:

$$G(s) = \frac{Te^{-sL_1}}{(T_1 s+1)(Ts+1)}, T_1 + L_1 = 1, T = 1, 2, 5, 10, \tag{A.1g}$$

$L_1 = 0.01, 0.02, 0.05, 0.1, 0.3, 0.5, 0.7, 0.9, 1$

Models 114 to 124 in Figure 6:

$$G(s) = \frac{1-\alpha s}{(s+1)^3}, \tag{A.1h}$$

$\alpha = 0.1, 0.2, 0.3, 0.4, 0.5, 0.6, 0.7, 0.8, 0.9, 1, 1.1$

Models 125 to 134 in Figure 6:

$$G(s) = \frac{1}{(s+1)((sT)^2 + 1.4sT + 1)}, \tag{A.1i}$$

$T = 0.1, 0.2, 0.3, 0.4, 0.5, 0.6, 0.7, 0.8, 0.9, 1$